Technical Note

Evaluation of the Effects of Differences in Metal Artifact Type and Location on Image Quality in Computed Tomography Scans

Se-Won Lim, Woo-Keun Choi[1], Sungchul Kim

Department of Radiological Science, Gachon University Medical Campus, Hambangmoe-ro, Incheon, [1]Department of Radiation Oncology, Samsung Medical Center, Sungkyunkwan University School of Medicine, Seoul, Korea

Abstract

Artifacts in computed tomography scans distort anatomical information and prevent an accurate diagnosis. Therefore, this study aims to determine the most effective method for reducing metal-induced artifacts by evaluating the effects of the metal artifact type and location, and the tube voltage on the image quality. Fe and Cu wires were inserted into a Virtual Water™ phantom at 6.5 and 11 cm distances from the center point (DPs). The contrast-to-noise ratios (CNRs) and signal-to-noise ratios (SNRs) were calculated to compare the images. The results reveal higher CNRs and SNRs when using standard and Smart metal artifact reduction (Smart MAR) algorithms for Cu and Fe insertions, respectively. The standard algorithm leads to a higher CNR and SNR for Fe and Cu at DPs of 6.5 and 11 cm, respectively. The Smart MAR algorithm provides effective outcomes at voltages of 100 and 120 kVp for wires located at 11 and 6.5 cm DP, respectively. The most effective imaging conditions for MAR is generated by the Smart MAR algorithm with a tube voltage for 100 kVp for Fe located at a DP of 11 cm. MAR can be improved by setting suitable tube voltage conditions according to the type and location of inserted metal.

Keywords: Contrast-to-noise ratio, metal artifact, signal-to-noise ratio, smart metal artifact reduction algorithm, standard algorithm

Received on: 21-09-2022 **Review completed on:** 30-12-2022 **Accepted on:** 18-01-2023 **Published on:** 18-04-2023

Introduction

In computed tomography (CT), artifacts lower the image quality and prevent accurate diagnoses in clinical practice.[1] Metal pieces inserted into the human body have higher atomic numbers than those of bones and tissues, resulting in higher attenuation contrast during X-rays, leading to a cupping effect and metal artifacts, such as streaks or black holes.[2,3] Hence, metal artifacts lower the contrast resolution and distort the images, thereby preventing an accurate assessment of any region of interest (ROI) close to the metal.[4,5] Therefore, metal artifacts in CT images must be reduced.

Conventional methods to reduce metal artifacts in CT images include using a high-energy tube voltage, low pitch, small slice thickness, or image reconstruction using bone algorithms.[6-8] However, these methods produce limited image quality enhancement and have the disadvantage of increased radiation exposure,[9] which is particularly enhanced in pediatric CT compared with adult CT because of a child's higher sensitivity.[10] As a result, numerous technological advancements in software and hardware have been aimed at resolving these limitations.

Access this article online

Quick Response Code:

Website: www.jmp.org.in

DOI: 10.4103/jmp.jmp_87_22

The smart metal artifact reduction (Smart MAR) algorithm, a well-known software-focused method, reduces metal artifacts in CT images. In this method, X-rays generated from a source penetrate the target object and produce a sinogram as raw attenuated data. Subsequently, the images are reconstructed to isolate the sinogram of metals from the original sonogram; thus, images with reduces artifacts can be obtained from the images of an area with a metal artifact with repeated reconstruction.[8] Numerous studies have applied the Smart MAR algorithm because of its outstanding results, and follow-up studies are ongoing. This method was developed to reduce the beam hardening effect through postprocessing.[11]

Metal artifacts vary in their effects on CT images based on the density, size, and location of the metal inserted into the human

Address for correspondence: Prof. Sungchul Kim, Department of Radiological Science, Gachon University Medical Campus, 21936, 191 Hambangmoe-ro, Incheon, Republic of Korea.
E-mail: ksc@gachon.ac.kr

How to cite this article: Lim SW, Choi WK, Kim S. Evaluation of the effects of differences in metal artifact type and location on image quality in computed tomography scans. J Med Phys 2023;48:80-4.

body. In the present study, metals with different densities were inserted into a tomotherapy cheese phantom at various distances from the center point (DPs), with different imaging conditions were used to determine their effects on the scan images. Furthermore, the levels of MAR with the standard and Smart MAR algorithms were compared with respect to the metal type.

In practice, noise signals in quantitative analyses indicate signal uncertainty and inaccuracy. As the measurement and analysis of noise signals are critical in evaluating image quality, this study used the signal-to-noise ratio (SNR) and contrast-to-noise ratio (CNR) as objective evaluation methods rather than using a subjective evaluation method to investigate the image quality.[12,13] Hence, the CNRs and SNRs were used as objective indicators of image analysis for comparisons between the metal types and locations, tube voltages, and algorithms to identify the most effective imaging conditions for MAR based on the metal type and location as well as the most effective conditions for the applying the Smart MAR algorithm. Thus, this study compared the effects of the type and location of metal objects inserted into the human body on CT scan images with respect to potential clinical application and determined the optimal imaging conditions for the Smart MAR algorithm.

Materials and Methods

Experimental devices and materials

CT scans were performed using a four-dimensional CT simulator (Discovery™ RT, NYSE, GE). The density of each metal was measured using a cylindrical form of the Virtual Water™ phantom (Gammex RMI, Middleton, WI) with 20 holes [Figure 1], and various metal types, imaging conditions, and DPs were investigated. The metal pieces were bundles of 20 Fe (7.87 g/cm^3) or Cu (8.94 g/cm^3) wires that were 1 mm in diameter. A fixture device used in radiation therapy, known as an MeV-Green (Jeonseong Medical, Co., Ltd.), was prepared [Figure 1] to remove the air in the margin that entered during the insertion of the metal in the hole of the Virtual Water™ phantom and fix the Fe or Cu wires at the center.

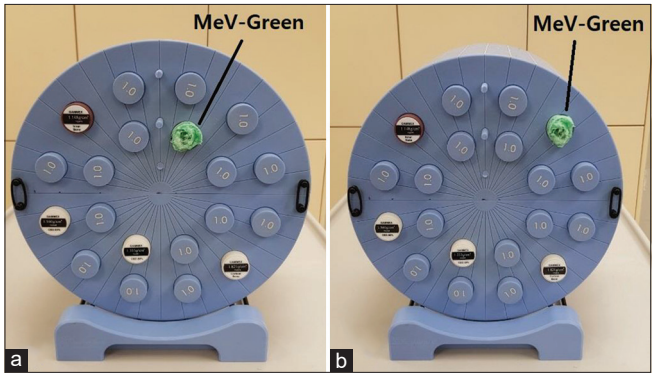

Figure 1: Distances from the center point. (a) 6.5 cm and (b) 11 cm from the center

Methods

Test conditions

The basic test conditions for the imaging included: display field of view of 50 cm, tube current of 350 mA, slice thickness of 2.5 mm, and scan range of superior 200 cm – inferior 200 cm. For each metal artifact type (Fe and Cu), the DP was set to 6.5 and 11 cm. In addition, the tube voltage was set to 100 (pediatric CT) or 120 kVp (adult CT) based on the CT scan conditions used at a hospital.

Image analysis

Using the standard and Smart MAR algorithms, image reconstruction was performed for each image obtained per metal type, DP, and tube voltage. Image J (Java 1.8.0_172, NIH) was used to evaluate the image quality for each condition, with the background and ROI set to 2.44 × 2.44 cm^2 and the ROI positioned below each metal image. After each domain was selected, the image that most clearly visualized the metal artifacts was selected across the 161 images obtained for each condition. For the 106th image, the CNR and SNR were calculated as follows.[14,15] The average value was determined by repeatedly measuring all values 10 times.

$$CNR = \left| \frac{(\text{Background SI}_{Avg} - \text{ROI SI}_{Avg})}{\sqrt{\text{Background SD}^2 - \text{ROI SD}^2}} \right| \quad (1)$$

$$SNR = \left| \frac{(\text{Background SI}_{Avg} - \text{ROI SI}_{Avg})}{\text{ROI SD}} \right| \quad (2)$$

where Background SI$_{Avg}$: The average intensity of the background signal; ROI SI$_{Avg}$: The average intensity of the ROI signal; ROI SD$_{Avg}$: Standard deviation of the intensity of the ROI signal; Background SD: Standard deviation of the intensity of the background signal.

Results

Contrast-to-noise ratio and signal-to-noise ratio with standard algorithm

The image quality according to the metal type (Fe or Cu) was evaluated at identical DPs and tube voltages. Compared with Fe, Cu exhibited CNR and SNR increases of 1.73–6.08 and 2.19–7.55, respectively.

When the tube voltage was increased from 100 to 120 kVp, the levels of increase in both the CNR and SNR were higher for Cu, with CNR and SNR increases of 1.54–2.21 and 1.58–2.33, for Fe, and 4.34–4.72 and 4.70–5.29, for Cu, respectively.

Regarding the change in image quality according to the DP for identical metal type and tube voltages, Fe exhibited decreased CNRs and SNRs with an increased DP, whereas Cu exhibited increases in both the CNRs and SNRs [Table 1 and Figure 2].

Contrast-to-noise ratio and signal-to-noise ratio for with smart metal artifact reduction algorithm

The image quality according to the metal type (Fe or Cu) was evaluated at identical DPs and tube voltages. Compared with

Table 1: Contrast-to-noise ratios and signal-to-noise ratios with standard algorithm

Metal	Density (g/cm^3)	Distance from center point (cm)	Tube voltage (kVp)	ROI SI_{Avg}	ROI SD	BKG SI_{Avg}	BKG SD	CNR	SNR
Fe	7.87	6.5	100	−7.251	181.107	−966.493	64.082	4.99	5.30
			120	−14.963	140.242	−979.304	46.404	6.53	6.88
		11	100	−46.133	255.302	−971.477	65.648	3.51	3.62
			120	−26.2	160.478	−980.864	45.679	5.72	5.95
Cu	8.96	6.5	100	23.702	131.826	−963.848	65.08	6.72	7.49
			120	19.002	82.346	−984.518	38.101	11.06	12.19
		11	100	23.549	119.987	−961.816	70.413	7.08	8.21
			120	16.093	74.011	−982.96	41.154	11.80	13.50

BKG: Background, SNR: Signal-to-noise ratio, CNR: Contrast-to-noise ratio, SI_{Avg}: The average intensity of the signal, ROI: Region of interest, SD: Standard deviation

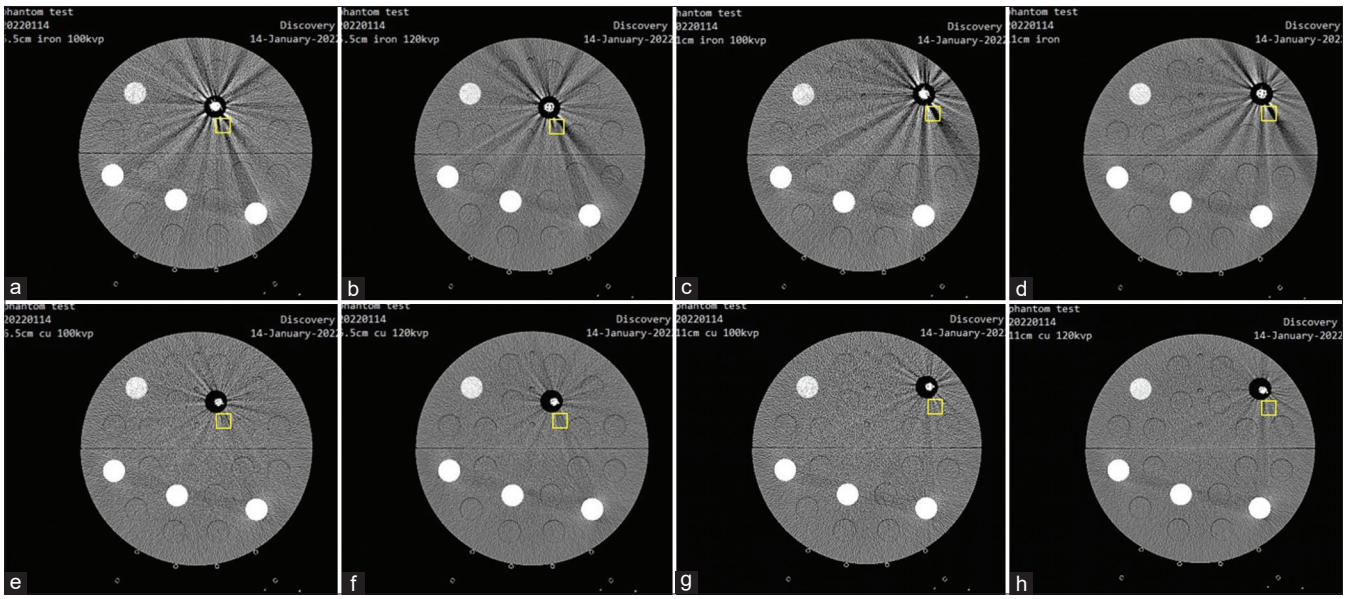

Figure 2: Standard algorithm images: a) Fe at 6.5 cm, 100 kVp, b) Fe at 6.5 cm, 120 kVp, c) Fe at 11 cm, 100 kVp, d) Fe at 11 cm, 120 kVp, e) Cu at 6.5 cm, 100 kVp, f) Cu at 6.5 cm, 120 kVp, g) Cu at 11 cm, 100 kVp, and h) Cu at 11 cm, 120 kVp

Cu, Fe exhibited CNR and SNR increases of 0.66–4.95 and 0.88–4.66, respectively, in contrast to the trend observed with the standard algorithm.

When the tube voltage was increased from 100 to 120 kVp, the CNRs and SNRs increased for both metals, by 11.77–12.59 and 10.94–13.89 for Fe and 12.10–16.06 and 12.51–17.67 for Cu, respectively.

The image quality (CNR and SNR) did not exhibit notable trends in relation to the DP for identical metal types and tube voltages [Table 2 and Figure 3].

Comparative analysis of images according to the algorithm

For both Fe and Cu insertions, the CNRs and SNRs were higher in the images obtained using the Smart MAR algorithm.

Compared with the standard algorithm, the Smart MAR algorithm exhibited higher increases in the CNRs and SNRs for Fe insertion than those for Cu insertion when evaluating the level of image quality enhancement per metal type, DP, and tube voltage. The imaging condition with the strongest MAR with the Smart MAR algorithm was Fe located at a DP of 11 cm, whereas that with the lowest effect was Cu, located at a DP of 11 cm [Table 3].

Discussion

This study investigated metal artifacts that interfere with imaging diagnosis by evaluating the effects of the metal type and location, tube voltage, and specific algorithms on the image quality.

First, CT scan images compared according to the metal type revealed higher CNRs and SNRs for inserted Cu when using the standard algorithm, whereas higher CNRs and SNRs were observed for Fe insertion when using the Smart MAR algorithm.

Comparing images with different metal locations revealed higher CNRs and SNRs when using the standard algorithm for DPs of 6.5 and 11 cm for Fe and Cu, respectively. In contrast, the CNRs and SNRs when using the Smart MAR

Table 2: Contrast-to-noise ratio and signal-to-noise ratio with smart metal artifact reduction algorithm

Metal	Density (g/cm^3)	Distance from center point (cm)	Tube voltage (kVp)	ROI SI_{Avg}	ROI SD	BKG SI_{Avg}	BKG SD	CNR	SNR
Fe	7.87	6.5	100	23.011	28.044	−981.792	24.408	27.03	35.83
			120	19.73	21.519	−986.763	13.5	39.62	46.77
		11	100	19.853	29.36	−983.32	18.6	28.86	34.17
			120	13.941	20.834	−987.266	13.157	40.63	48.06
Cu	8.96	6.5	100	26.778	31.404	−981.834	24.189	25.44	32.12
			120	19.357	22.627	−990.502	14.547	37.54	44.63
		11	100	24.549	34.099	−981.696	24.672	23.91	29.51
			120	15.666	21.262	−987.448	13.338	39.97	47.18

BKG: Background; SNR: Signal-to-noise ratio; CNR: Contrast-to-noise ratio; SI_{Avg}: The average intensity of the signal, ROI: Region of interest, SD: Standard deviation

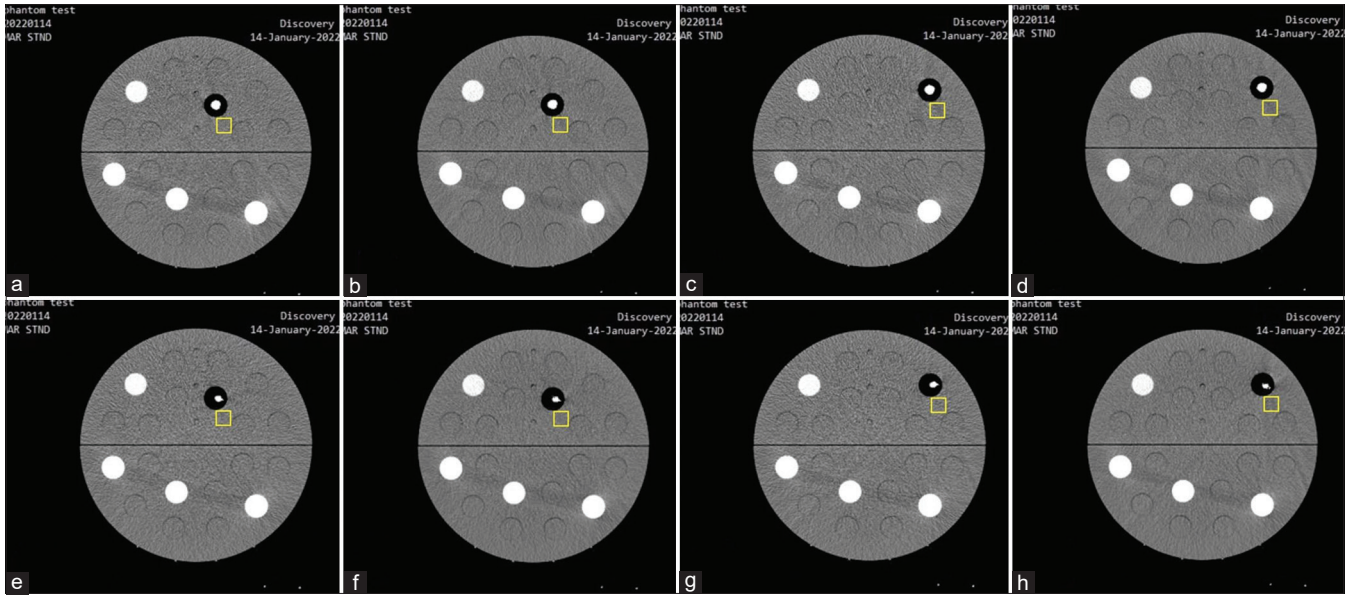

Figure 3: Smart metal artifact reduction algorithm images: (a) Fe at 6.5 cm, 100 kVp, (b) Fe at 6.5 cm, 120 kVp, (c) Fe at 11 cm, 100 kVp, (d) Fe at 11 cm, 120 kVp, (e) Cu at 6.5 cm, 100 kVp, (f) Cu at 6.5 cm, 120 kVp, (g) Cu at 11 cm, 100 kVp, and (h) Cu at 11 cm, 120 kVp

algorithm were higher for a DP of 6.5 cm with a low tube voltage, and a DP of 11 cm, with a high tube voltage for both Fe and Cu.

Comparing images obtained when using different tube voltages revealed higher CNRs and SNRs for both metals as the voltage increased, irrespective of the algorithm. Increasing the tube voltage led to considerable increases in the CNR and SNR at a DP of 11 cm compared those at 6.5 cm. Therefore, an increased tube voltage was more effective in MAR for metal pieces located far from the center point than for those located close to the center point.

For both Fe and Cu, the images obtained using the Smart MAR algorithm revealed higher CNRs and SNRs than those obtained using the standard algorithm. Increasing the tube voltage for conventional MAR is limited because of the increased radiation exposure, whereas the Smart MAR algorithm achieves MAR without increasing the radiation exposure.[16]

The imaging condition with the highest MAR with the Smart MAR algorithm was Fe at a DP of 11 cm. For reducing metal artifacts using the Smart MAR algorithm, a low tube voltage is effective when the metal is located far from the center point, while a high tube voltage is effective when the metal is located close to the center point.

In the case of Fe insertion, more metal artifacts were detected; however, the image reconstruction using the Smart MAR algorithm was highly effective in reducing the metal artifacts.

The imaging conditions for the highest CNRs and SNRs were similar to those obtained by Luca *et al*.,[17] with image reconstruction using the Smart MAR algorithm with Fe at a DP of 11 cm and a tube voltage of 120 kVp. The conditions with the lowest CNRs and SNRs corresponded to those of image reconstruction using the standard algorithm with Fe at a DP of 11 cm and a tube voltage of 100 kVp.

Thus, the results of this study suggested that CT scan image quality is determined not by a single factor but by a combination of factors, including the metal type, and location, algorithm, and tube voltage.

Table 3: Ratios of contrast-to-noise ratio and signal-to-noise ratio values with the smart metal artifact reduction and standard algorithms

Material	Distance from center point (cm)	Tube voltage (kVp)	Smart MAR/ standard algorithm	
			CNR	SNR
Fe	6.5	100	5.41	6.76
		120	6.07	6.8
	11	100	8.22	9.43
		120	7.1	8.08
Cu	6.5	100	3.79	4.29
		120	3.39	3.66
	11	100	3.38	3.59
		120	3.39	3.5

SNR: Signal-to-noise ratio, CNR: Contrast-to-noise ratio, MAR: Metal artifact reduction

This study has several limitations. First, the most used material for artificial joints is titanium alloy, but its processing was unsuitable for the experiment; thus Fe and Cu were used. In the future, experiments using various types of materials, such as titanium alloys and polyethylene, will be necessary. In addition, other quality evaluation methods should be investigated, including their corresponding SNRs and CNRs.

Conclusions

The standard algorithm exhibited higher CNRs and SNRs for Cu insertion, whereas the Smart MAR algorithm exhibited higher CNRs and SNRs for Fe insertion. In the standard algorithm, the CNRs and SNRs were higher for Fe at a closes DP and for Cu at a farther DP. The conditions for effective MAR using the Smart MAR algorithm were a tube voltage of 100 kVp for metals located far from the center point and 120 kVp for metals located close to the center point. The optimal imaging conditions with the highest MAR were the Smart MAR algorithm for Fe at a far DP and a tube voltage of 100 kVp. Therefore, selecting the appropriate tube voltage depending on the type and depth of metal inserted into the human body may affect the reduction of artifacts.

Financial support and sponsorship

Nil.

Conflicts of interest

There are no conflicts of interest.

References

1. Jeon S, Lee CO. A CT metal artifact reduction algorithm based on sinogram surgery. J Xray Sci Technol 2018;26:413-34.
2. Goo EH. A study of the CT MAR using single-source and dual-source devices: Practical comparison using animal phantom fabrication. J Korean Soc Radiol 2020;14:1003-11.
3. Hur J, Kim D, Shin YG, Lee H. Metal artifact reduction method based on a constrained beam-hardening estimator for polychromatic x-ray CT. Phys Med Biol 2021;66:065025.
4. Lee MJ, Kim S, Lee SA, Song HT, Huh YM, Kim DH, *et al.* Overcoming artifacts from metallic orthopedic implants at high-field-strength MR imaging and multi-detector CT. Radiographics 2007;27:791-803.
5. Link TM, Berning W, Scherf S, Joosten U, Joist A, Engelke K, *et al.* CT of metal implants: Reduction of artifacts using an extended CT scale technique. J Comput Assist Tomogr 2000;24:165-72.
6. Glover GH, Pelc NJ. An algorithm for the reduction of metal clip artifacts in CT reconstructions. Med Phys 1981;8:799-807.
7. Brooks RA, Di Chiro G. Beam hardening in x-ray reconstructive tomography. Phys Med Biol 1976;21:390-8.
8. Ling CC, Schell MC, Working KR, Jentzsch K, Harisiadis L, Carabell S, *et al.* CT-assisted assessment of bladder and rectum dose in gynecological implants. Int J Radiat Oncol Biol Phys 1987;13:1577-82.
9. Park KS, Choi WJ, Kim DH. A study of the metal artifact reduction using dual energy CT: Clinical applications of dual energy and MAR algorithm. J Korean Soc Radiol 2021;15:273-79.
10. Lee J, Jang SJ, Jang YI. Medical radiation exposure in children CT and dose reduction. J Korea Contents Assoc 2014;14:356-63.
11. Kim HJ. Usefulness evaluation of application of metallic algorithm reducing for beam hardening artifact occur in typical brain CT image. J Korean Soc Radiol 2018;12:389-95.
12. Kim JM, Min JW, Jeong HW, Im EG, Yang HJ. The noise evaluation for REGIUS 150 CR system. J Radiol Sci Technol 2006;29:237-40.
13. Seo YH. Song JN. Analysis of the ESD and DAP according to the change of the cine imaging condition of coronary angiography and usefulness of SNR and CNR of the images: Focusing on the change of tube current. J Korean Soc Radiol 2019;13:371-79.
14. Son SY, Choi KW, Min JW, Son JH, Kim KW, Jung JH, *et al.* Evaluation of quantitative on T-spine exhalation technique and T-spine breathing technique of natural breathing. J Korea Acad Ind Coop Soc 2013;14:4429-36.
15. Cho PK. Comparative evaluation of images after applying quantum denoising system algorithm to brain computed tomography. J Radiol Sci Technol 2017;40:589-94.
16. Kim HJ, Yoon J. Analysis of the artifact reduction rate for the types of medical metals in CT with MAR algorithm. J Korea Acad Ind Coop Soc 2016;17:655-62.
17. Ceccarelli L, Vara G, Ponti F, Miceli M, Golfieri R, Facchini G. Reduction of metal artifacts caused by titanium peduncular screws in the spine by means of monoenergetic images and the metal artifact reduction software in dual-energy computed tomography. J Med Phys 2022;47:152-8.